Thermochimica Acta, 191 (1991) 285–291
Elsevier Science Publishers B.V., Amsterdam

Synthesis and thermal decomposition of UO_2(II) complexes with 4,6-dihydroxycoumaran-3-one and *O*-vanillin oxime

M.L. Dhar [1] and Onkar Singh

Department of Chemistry, Jammu University, Jammu-180 004 (India)

(Received 29 March 1991)

Abstract

The synthesis, nature and an evaluation of thermal decomposition kinetic parameters (E, Z, ΔS^*) of the complexes of U(VI) with 4,6-dihydroxycoumaran-3-one and *O*-vanillin oxime are reported and discussed on the basis of elemental analysis, IR, electronic spectral and thermoanalytical studies. The complexes are found to have the compositions $[UO_2(C_8H_5O_4)_2 \cdot 2C_2H_5OH]$ and $[UO_2(C_8H_8NO_3)_2 \cdot 2H_2O]$ with distorted octahedral symmetry and the mechanism of thermal decomposition is of the random nucleation type.

INTRODUCTION

4,6-Dihydroxycoumaran-3-one and *O*-vanillin oxime have been reported to give colour reactions with uranyl ion [1]. It was therefore considered interesting to study in detail the nature and thermal decomposition of the complexes formed in the solid state.

EXPERIMENTAL

4,6-Dihydroxycoumaran-3-one [2,3] and *O*-vanillin oxime [4,5] were prepared by known methods. The complexes were prepared by refluxing the uranyl nitrate and the ligand (M : L = 1 : 10) in ethanol. The precipitated complexes were washed free of excess of ligand with acetone and dried in vacuum over anhydrous calcium chloride. Carbon, hydrogen and metal contents were estimated by a micro-analytical method; IR spectroscopy (4000–200 cm^{-1}) and DRS (50000–10000 cm^{-1}) were carried out using a Perkin Elmer 377 grating IR spectrophotometer and a VSU2P (Carl-Zeiss) spectrophotometer respectively.

The thermal decomposition studies of the complexes were done using a Paulik–Paulik MOM derivatograph (Hungary) [6] for the simultaneous DTA and TGA using α-alumina as the reference material and a heating

---

[1] Author to whom correspondence should be addressed.

0040-6031/91/$03.50 © 1991 – Elsevier Science Publishers B.V. All rights reserved

rate of 10 °C min^{-1}. The kinetics of thermal decomposition of the complexes were investigated by the non-isothermal methods of Piloyan et al. [7], Coats and Redfern [8] and Horowitz and Metzger [9]. The values obtained from the Piloyan et al. and Coats–Redfern methods were plotted against T^{-1}. In the case of the Horowitz–Metzger method, values obtained were plotted against θ_1 ($\theta_1 = T - T_m$, where T_m is peak temperature). These plots were analysed for various values of the kinetic parameters.

RESULTS AND DISCUSSION

The elemental analyses for the complexes give the metal, carbon and hydrogen content values well in conformity with the calculated values for the compositions (see Table 1).

The nature of the complexes is supported by IR spectral studies [10,11]. 4,6-Dihydroxycoumaran-3-one shows ν(O–H), ν(C=O) and ν(O–C) stretchings at 3520, 1670 and 1070 cm^{-1} respectively and *O*-vanillin oxime shows ν(O–H) and ν(C=N + C–C) stretchings at 3350 and 1625 cm^{-1} respectively. These values shift to lower values on complexation with metal ion. The bands due to ν(O–H) stretching disappear as the proton gets abstracted. Additional bands in the $[(UO_2(C_8H_5O_4)_2 \cdot 2C_2H_5OH]$ spectrum at 1150, 825 and 700 cm^{-1} corresponding to ν(M–O) and ν(M–O + C–C) are observed. Similarly additional bands in the $[UO_2(C_8H_8NO_3)_2 \cdot 2H_2O]$ spectrum at 1040 and 760 cm^{-1} corresponding to ν(M–O) and ν(M–O + C–C) are observed.

The electronic absorption spectra reveal the nature of the complexes. The complexes show bands at 40816, 25000 and 20000 cm^{-1}. U(VI) with its 5f^0 electronic configuration has no 5f → 5f or 5f → 6d transitions [12–15]; the appearance of bands in their reflectance spectra can therefore be assigned to electron transfer bands. These charge transfer bands suggest distorted octahedral structures for the complexes.

The TG curve (Fig. 1) shows that the complex $[UO_2(C_8H_5O_4)_2 \cdot 2C_2H_5OH]$ starts decomposing at 333 K; this continues up to 503 K and corresponds to the loss of the two coordinated ethanol molecules. The residual complex further decomposes at 508 K up to 835 K when no further loss in mass is noted; this corresponds to the loss of the ligand moiety. One endothermic peak at 403 K in connection with the loss of ethanol molecules

TABLE 1

Elemental analyses (observed %/calculated %)

Complex	Metal	Carbon	Hydrogen	Nitrogen
$[UO_2(C_8H_5O_4)_2 \cdot 2C_2H_5OH]$	39.0/38.5	39.0/38.7	3.0/2.8	–
$[UO_2(C_8H_8NO_3)_2 \cdot 2H_2O]$	36.8/37.1	29.4/30.3	3.5/3.1	5.0/4.4

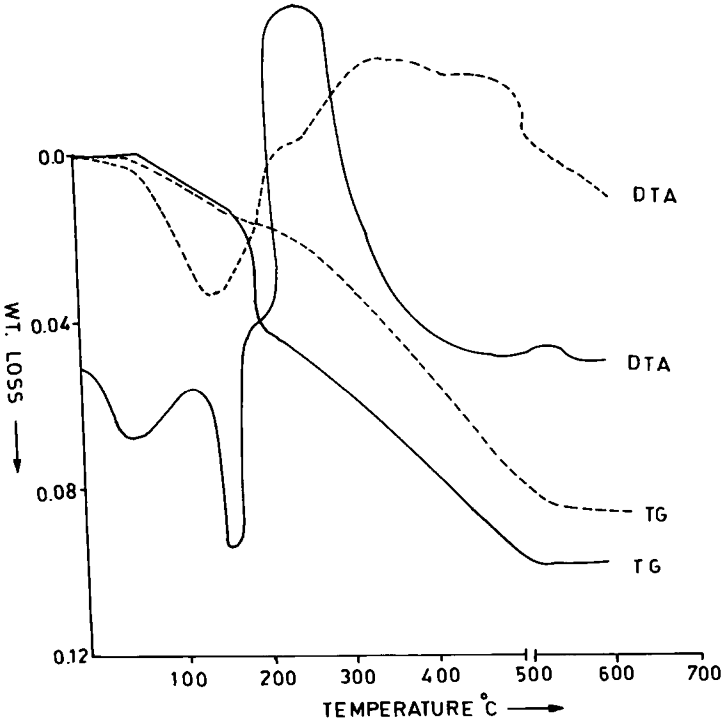

Fig. 1. Simultaneous TG–DTA curves: — — —, $[UO_2(C_8H_5O_4)_2 \cdot 2C_2H_5OH]$ (1); ——, $[UO_2(C_8H_8NO_3)_2 \cdot 2H_2O]$ (2).

and one exothermic peak at 663 K in connection with the loss of the ligand moiety from the DTA curve are observed.

Similarly the complex $[UO_2(C_8H_8NO_3)_2 \cdot 2H_2O]$ starts decomposing at 313 K; this continues up to 468 K and corresponds to the loss of the two coordinated water molecules as indicated by the two endothermic peaks at 340 and 443 K from the DTA curve (Fig. 1). The complex further decomposes at 473 K continuing up to 823 K when no further loss in mass is noted. This mass loss is equal to the loss of the ligand moiety; corresponding to this, one exothermic peak is observed at 540 K in the DTA curve. The oxide, U_3O_8 is formed as the end product in both cases.

Non-isothermal kinetics of the first steps have been studied. From the values of α (the fractional mass loss), the corresponding $(1-\alpha)^n$ values were calculated where n depends upon the reaction model. The corresponding values of $g(\alpha) = \mathrm{d}\int_0^{\alpha}(\alpha)$ were calculated for the equations of Piloyan et al. [7], Coats and Redfern [8] and Horowitz and Metzger [9] with different values of n. Plots giving the best linear fits were as follows: $\log \alpha/T^2$ vs. T^{-2} (Fig. 2) for equations of Piloyan et al. [7]; $\log(-\ln((1-\alpha)/T^2))$ vs. T^{-1} (Fig. 2) for equations of Coats and Redfern [8]; and $\log(-\ln(1-\alpha))$ vs. θ_1 (Fig. 3) for equations of Horowitz and Metzger [9].

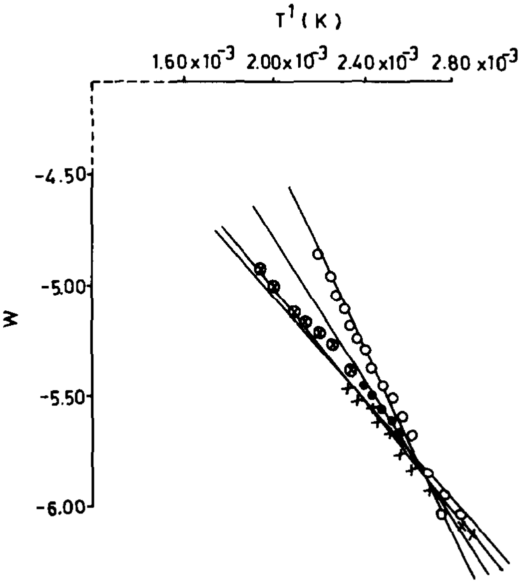

Fig. 2. Piloyan et al. [7] plots: *, complex (1) and ×, complex (2) when $W = \log \alpha / T^2$. Coats and Redfern [8] plots: ⊙, complex (1) and *, complex (2) when $W = \log[-\ln((1-\alpha)/T^2)]$.

This suggests a random nucleation mechanism. The plots of α–T (K) (Fig. 4) for both complexes are of the same pattern and also suggest a random nucleation mechanism [16]. The curves with an acceleratory period without any apparent induction period thus indicate that no surface nucleation or branching occurs during the first step of decomposition.

The values of slope, intercept and energy of activation were obtained from Figs. 2 and 3. The values of Z in the case of Piloyan et al. and Coats and Redfern were obtained by employing eqn. (1), while the values of Z in

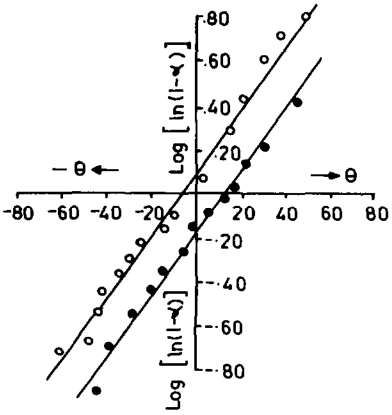

Fig. 3. Horowitz and Metzger [9] plots: o, complex (1) and •, complex (2).

TABLE 2

Decomposition kinetics parameters and nucleation mechanism

Complex	Step	Equation	E (kJ mol^{-1})	Z (s^{-1})	ΔS^* (J K^{-1} mol^{-1})	Mechanism
$[UO_2(C_8H_8NO_3)_2 \cdot 2H_2O]$	First	Piloyan et al. [7]	30.08	13.50	−98.08	
$[UO_2(C_8H_5O_4)_2 \cdot 2C_2H_5OH]$	First	Piloyan et al. [7]	22.97	1.03		
$[UO_2(C_8H_8NO_3)_2 \cdot 2H_2O]$	First	Coats and Redfern [8]	40.68	538.88	−84.77	RN [a]
$[UO_2(C_8H_5O_4)_2 \cdot 2C_2H_5OH]$	First	Coats and Redfern [8]	23.56	1.24	−106.91	RN [a]
$[UO_2(C_8H_8NO_3)_2 \cdot 2H_2O]$	First	Horowitz and Metzger [9]	47.34	6.23×10^{-3}	−125.81	RN [a]
$[UO_2(C_8H_5O_4)_2 \cdot 2C_2H_5OH]$	First	Horowitz and Metzger [9]	100.77	12.6×10^{-3}	−91.91	RN [a]

[a] RN random nucleation mechanism.

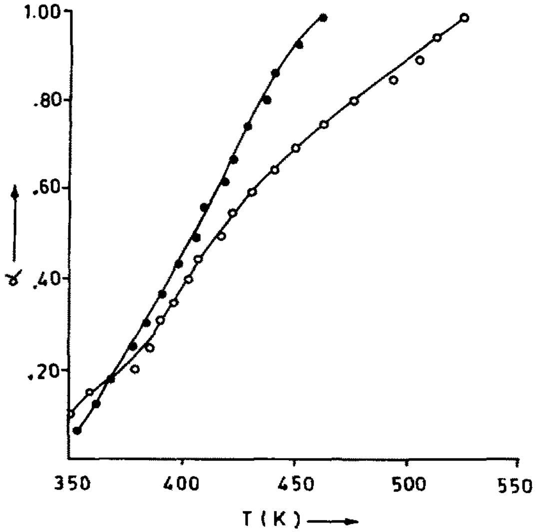

Fig . 4. $\alpha - T$(K) graphs: ●, complex (1) and ○, complex (2).

the case of Horowitz and Metzger were obtained by employing eqn. (2). The entropies of activation (ΔS^*) were calculated using eqn. (3)

$$\text{Intercept} = \log\frac{ZR}{\beta E} \tag{1}$$

$$Z = \frac{E}{RT_\text{m}}\beta \exp\left(\frac{E}{RT_\text{m}^2}\right) \tag{2}$$

$$Z = \frac{KT_\text{m}}{h} \exp\left(\frac{\Delta S^*}{R}\right) \tag{3}$$

where R represents the molar gas constant, β the rate of heating (K s^{-1}), K is the Boltzmann constant and h is Planck's constant (see Table 2).

From the above discussion it is concluded that 4,6-dihydroxycoumaran-3-one and *O*-vanillin oxime behave as bidentate ligands. The complexes decompose in two well-defined steps involving a random nucleation mechanism, forming U_3O_8 as the end product.

REFERENCES

1 R.K. Raina, Ph.D. Thesis, Jammu University, India, 1979.
2 D.M. Fitzgerald, J.F.C. Sullivan, E.M. Phillun and T. Swheeler, J. Chem. Soc., (1955) 860.
3 A.C. Jain and V.K. Rohtgi, Indian J. Chem., 7 (1969) 6.
4 D.P. Goel, K.C. Trikha and R.P. Singh, Indian J. Appl. Chem., 32 (1969) 62.
5 A.I. Vogel, Quantitative Organic Analysis, Longman Green, London, 1962, p. 571.
6 F. Paulik, J. Paulik and L. Erdey, Z. Anal. Chem., 160 (1958) 241.

7 G.O. Piloyan, I.D. Ryabchikov and O.S. Novikova, Nature, 212 (1966) 1229.
8 A.W. Coats and J.P. Redfern, Nature, 68 (1964) 101.
9 H. Horowitz and G. Metzger, Anal. Chem., 35 (1963) 1464.
10 K. Nakamoto, Infra-red Spectra of Inorganic Coordination Compounds, 2nd Edn., Wiley, New York, 1971.
11 D.M. Admas, Metal Ligand and Related Vibrations, St. Martin's Press, London, 1967.
12 M. Bartusek and L. Sommer, J. Inorg. Nucl. Chem., 27 (1965) 2397.
13 J.C. Bailar, H.J. Emeleus, Sir Ronald Nyholm and A.F.T. Dickenson (Eds.), Comprehensive Inorganic Chemistry, Vol. 5, Pergamon, Oxford 1973.
14 F.A. Cotton (Ed.), Progress in Inorganic Chemistry, Vol. 6, Wiley Interscience, 1964.
15 A.B.P. Lever, Inorganic Electron Spectroscopy, Elsevier, Amsterdam, 1968.
16 D.A. Young, in The International Encyclopaedia of Physical Chemistry, Solid and Surface Kinetics, F.C. Tompkins (Ed.), Vol. 1, Pergamon, London, 1966, p. 5.